

# Computer simulation of fatigue crack propagation under random loading conditions

A. Bacila<sup>a,b,\*</sup>, X. Decoopman<sup>a</sup>, R. Vatavu<sup>c</sup>, G. Mesmacque<sup>a</sup>, M. Voda<sup>a,b</sup>, V.A. Serban<sup>b</sup>

<sup>a</sup> Laboratoire de Mécanique de Lille, UMR CNRS 8107, IUT A GMP Le recueil, Rue de la recherche BP 179, 59653 Villeneuve d'Ascq, France

<sup>b</sup> Mechanical Faculty of Timisoara, Bd. Mihai Viteazu Nr.1, Timisoara 300222, Romania

<sup>c</sup> The "Stefan cel mare" University of Suceava, Universitatii 13, 720229 Suceava, Romania

Received 7 September 2006; received in revised form 16 February 2007; accepted 26 February 2007

Available online 14 March 2007

## Abstract

The aim of this study is to simulate fatigue crack propagation under random loading conditions using a simple algorithm based on the Wheeler model [Wheeler O. Spectrum loading and crack growth. *J Basic Eng D* 1972;94:181–86]. To create the computer simulation, a model based on the mechanical properties of the material has been used. These properties include the yield stress ( $\sigma_y$ ) and Paris's constants  $C$  and  $m$ . The loading conditions (baseline loading ratio  $R$ , baseline stress intensity factor range  $\Delta K$  and overload stress intensity factor  $K_{o1}$ ,  $R_{o1}$ ) are also required. The present model is validated with fatigue crack growth test data conducted on 12NC6 steel samples with four different heat treatments in order to have different types of mechanical behavior. The computer simulation and experimental results for crack propagation for different overload distributions (a single overload, a repeated overload, different overload magnitudes, random overload) are in good agreement.

© 2007 Elsevier Ltd. All rights reserved.

**Keywords:** Fatigue crack propagation; Overload; Random loading; Computer simulation

## 1. Introduction

While periodic maintenance inspection programs are vital for the prevention of critical failures, they are both costly and time consuming. Even an overload test with a single overload takes about 20 h.

In particular, fatigue tests are very expensive, since they require a lot of human and machine time, so it is very important to find models and develop suitable software in order to simulate fatigue analyses.

A number of models for performing broad-spectrum fatigue analyses have been proposed, including non-linear damage summation models [2,3], strain–energy methods [4,5] and models that use modified strain–life curves together with a linear damage rule [6–8]. The major short-

coming of many of these models is that they are often material-specific and are therefore unsuitable for incorporation into computer simulation programs for general use.

We decided to solve the problem of predicting crack propagation evolution with simple software that does not need performant computer resources, but uses a simple mathematical model based on a traditional approach that can also reproduce the behavior of a structure in the case of different overload distributions.

The software can run various types of overload conditions.

Many experimental results have been compared with the simulated results. This comparison shows a good agreement.

## 2. Experiments

In order to establish a model for the initial delay in crack evolution in the case of overload, compact tension (CT) specimens, 15 mm wide and 80 mm long, made of

\* Corresponding author. Address: Laboratoire de Mécanique de Lille, UMR CNRS 8107, IUT A GMP Le recueil, Rue de la recherche BP 179, 59653 Villeneuve d'Ascq, France.

E-mail address: [bacila@ed.univ-lille1.fr](mailto:bacila@ed.univ-lille1.fr) (A. Bacila).

**Nomenclature**

$a$	crack length (mm)	$K_{2ol}$	stress intensity factor for the second overload (MPa $\sqrt{m}$ )
$a_{ol}$	crack length where the overload was applied (mm)	$N$	number of cycles
$a_d$	crack length affected by overload (mm)	$R$	baseline stress intensity factor ratio ( $=K_{min}/K_{max}$ )
$a_{min}$	crack length associated with the minimum crack growth rate (mm)	$R_{ol}$	overload ratio ( $=K_{ol}/K_{max}$ )
$C, m$	Paris's constants	$\sigma_y$	material yield stress (MPa)
$\Delta K$	baseline stress intensity factor range ( $=K_{max} - K_{min}$ ) (MPa $\sqrt{m}$ )	$\omega_{ol}^m$	overload monotonic plastic zone $= \alpha (K_{ol}/\sigma_y)^2$ (mm)
$K_{ol}$	stress intensity factor for overload (MPa $\sqrt{m}$ )	$\omega_{ol}^c$	overload cyclic plastic zone $= \alpha ((K_{ol} - K_{min})/2\sigma_y)^2$ (mm)
$K_1$	stress intensity factor for the first crack propagation (MPa $\sqrt{m}$ )	$\omega_{base}^m$	baseline monotonic plastic zone $= \alpha (K_{max}/\sigma_y)^2$ (mm)
$K_{1ol}$	stress intensity factor for the first overload (MPa $\sqrt{m}$ )	$\omega_{base}^c$	baseline cyclic plastic zone $= \alpha (\Delta K/2\sigma_y)^2$ (mm)
$K_2$	stress intensity factor for the second crack propagation (MPa $\sqrt{m}$ )	$S_r$	severity ratio $\left( = \frac{(da/dN)_{min}}{(da/dN)_{base}} \right)$

12NC6 steel were used. The dimensions of the samples are in accordance with the prescription ASTM E647 as in Fig. 1.

Four different heat treatments were selected in order to obtain four different types of mechanical behavior. Each treatment begins with an austenization at 880 °C for 1 h. The subsequent treatments are as follows:

- Treatment TR300, which is quenching with water followed by tempering to 300 °C.
- Treatment TR500, which is quenching with water followed by tempering to 500 °C.
- Treatment NA (normalizing in air), which is cooling with air.
- Treatment NF (normalizing in the furnace), which is cooling in the furnace.

The mechanical characteristics of 12NC6 steel are displayed in Table 1.

Crack tests (constant amplitude and overload) were carried out using an INSTRON 8500 test machine with a capacity of  $\pm 100$  kN and a maximal frequency of 50 Hz.

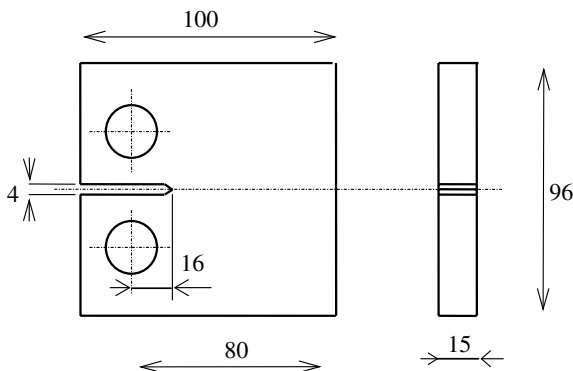


Fig. 1. Geometry of the samples (in mm).

These tests were carried out at room temperature. The test frequency was 30 Hz. The crack propagation length was measured on the front of the specimen. A binocular magnifying glass (20 $\times$ ) set on a micrometric table (50 mm stroke, 0.05 mm accuracy) was used. A camera views the other side of the specimen and thus enables the crack growth to be monitored. A stroboscopic lamp set at the fatigue test frequency allows the crack length to be measured.

The measurement of the crack closure is carried out on a 0.1 Hz frequency cycle. Data are recorded at each load adjustment as well as during pre-overload, during overload and post-overload cycles.

One of the objectives of this experimental study was to analyze the role of each plasticized zone in the delay in crack propagation.

It should be stressed that the loading parameters of in an overload test of the type defined here are determined by three values: two of these characterize the initial loading (the load ratio  $R$  and the baseline amplitude  $\Delta K$ ); the last relates to the amplitude of the overload (i.e., to the choice of  $K_{ol}$ ,  $R_{ol}$  or  $\tau_{ol}$ ). Each of these three values produces an effect on one or more of the plasticized zones (four in the case of a single overload):

- $\omega_{ol}^m = \alpha \cdot (K_{ol}/\sigma_y)^2$ : monotonic plastic zone of overload;
- $\omega_{ol}^c = \alpha \cdot (\Delta K_{ol}/2\sigma_y)^2$ : cyclic plastic zone of overload;
- $\omega_{base}^m = \alpha \cdot (K_{max}/\sigma_y)^2$ : monotonic plastic zone of basic loading;
- $\omega_{base}^c = \alpha \cdot (\Delta K/2\sigma_y)^2$ : cyclic plastic zone of basic loading.

The material becomes monotonically plasticized during the first part of the cycle (loading), whereas cyclic plasticization occurs during the second part of the cycle (unloading) on a material that is already plasticized. The design

Table 1  
Mechanical characteristics of 12NC6 steel

Heat treatment	$\sigma_{y0.2\%}$ (MPa)	$\sigma_{ult}$ (MPa)	$E$ (GPa)	Striction $Z$ (%)	Lenghtening $A$ (%)	$K$ (MPa)	$n$	$Hv_{(20)}$
NF	340	489	194	49	31.2	544	0.45	133
NA	330	710	208	62	21	1017	0.41	195
TR500	900	911	216	64	16	495	0.53	275
TR300	1005	1262	226	54	12	729	0.35	360

Table 2  
Loading conditions for a single overload

Heating treatment	$K_{max}$ (MPa $\sqrt{m}$ )	$K_{min}$ (MPa $\sqrt{m}$ )	$K_{ol}$ (MPa $\sqrt{m}$ )	$R$	$R_{ol}$
NF	22	2.2	44	0.1	2
NA	32.5	9.1	65	0.28	2
TR300	32.36	6.8	71.2	0.21	2.2
TR500	24	2.4	60	0.1	2.5

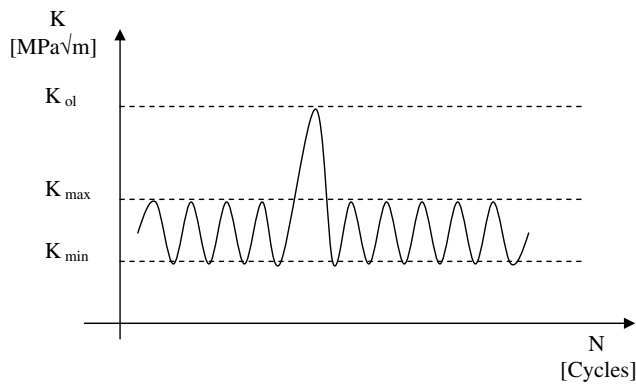


Fig. 2. Loading history for a single overload.

assumptions for the cyclic plasticized zones are based on a linear law of kinematic work hardening.

The parameters used for the case with one overload are presented in Table 2 and the loading history in Fig. 2.

The experimental results for crack length versus number of cycles for a single overload are presented in Fig. 3.

The parameters used for the case with two consecutive overloads are presented in Table 3 and the loading history in Fig. 4.

After the first overload, the initial crack speed was modified because the crack propagated too slowly, but this modification offered us the possibility to verify the computer simulation for various conditions of crack propagation.

The modifications of the initial crack speed give different slopes for the evolution of the speed curve. In our case, we have two different slope tendencies as presented in Fig. 5.

The second overload was applied when the crack started to grow inside the plastic zone created by the first overload, and only for the NF heat treatment.

### 3. Empirical model for fatigue crack propagation

The disturbance of the fatigue crack growth rate after overload is often described [20–22,24–26] starting from

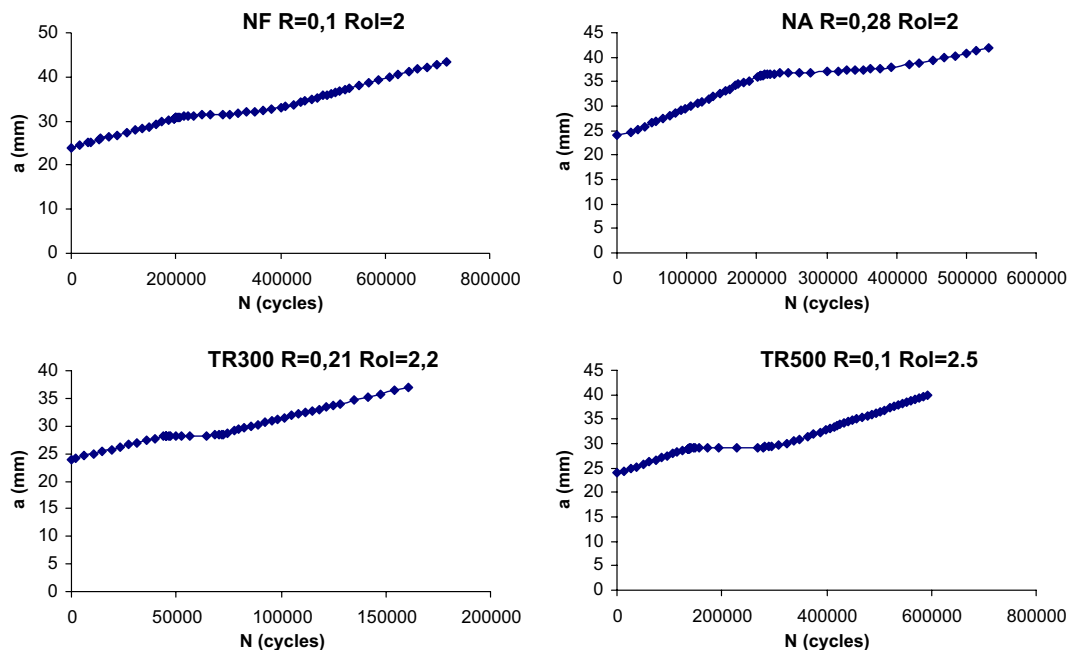


Fig. 3. Crack length  $a$  versus number of cycles  $N$  for a single overload.

Table 3  
Loading conditions for two consecutive overloads

Heating treatment	Before overload	First overload	After first overload	Second overload	After overloads
NF	$K_{1\max} = 22$ (MPa $\sqrt{\text{m}}$ ) $K_{1\min} = 11$ (MPa $\sqrt{\text{m}}$ ) $R = 0.5$	$K_{2\max} = 22$ (MPa $\sqrt{\text{m}}$ ) $K_{2\min} = 2.2$ (MPa $\sqrt{\text{m}}$ ) $K_{1\text{ol}} = 44$ (MPa $\sqrt{\text{m}}$ ) $R = 0.1$ $R_{\text{ol}} = 2$	$K_{2\max} = 22$ (MPa $\sqrt{\text{m}}$ ) $K_{2\min} = 2.2$ (MPa $\sqrt{\text{m}}$ ) $R = 0.1$	$K_{2\max} = 22$ (MPa $\sqrt{\text{m}}$ ) $K_{2\min} = 2.2$ (MPa $\sqrt{\text{m}}$ ) $K_{2\text{ol}} = 39.6$ (MPa $\sqrt{\text{m}}$ ) $R = 0.1$ $R_{\text{ol}} = 1.8$	$K_{2\max} = 22$ (MPa $\sqrt{\text{m}}$ ) $K_{2\min} = 2.2$ (MPa $\sqrt{\text{m}}$ ) $R = 0.1$

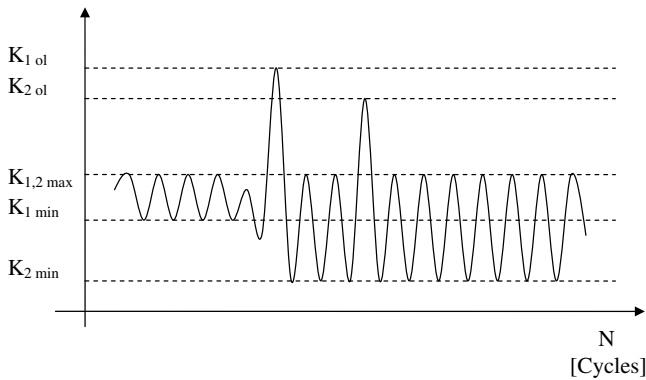


Fig. 4. Loading history for two consecutive overloads.

an equation introducing a delay coefficient  $C_d$ . The general expression can be written in the following form:

$$(da/dN)_d = C_d \cdot (da/dN)_{\text{base}} \quad (1)$$

The model is based on the following assumptions, which were confirmed at the time of our experimental study:

- the delay occurs at a distance after overload equal to the value of  $a_d$  which is estimated starting from the sizes of the monotonic plasticized zones of overload and basic load, and given by the following expression:

$$a_d = \frac{1}{2\pi} \left( \frac{K_{\max}}{\sigma_y} \right)^2 (R_{\text{ol}}^2 - 1) = \omega_{\text{ol}}^m - \omega_{\text{base}}^m \quad (2)$$

- the minimum speed is reached at a distance  $a_{\min}$ , which can be compared with the cyclic plasticized zone of overload

$$a_{\min} = \frac{1}{2\pi} \left( \frac{\Delta K_{\text{ol}}}{2\sigma_y} \right)^2 = \omega_{\text{ol}}^c \quad (3)$$

- the value of the minimum fatigue crack growth rate after overload  $(da/dN)_{\min}$  can be deduced starting from the severity ratio  $S_r$  which also utilizes the baseline fatigue crack growth rate  $(da/dN)_{\text{base}}$ . In this study, the severity ratio is given by the following relation:  $S_r = 7.10^{12} \times (\tau_{\text{ol}})^{-6}$ . Fig. 6 gives a schematic indication of the various assumptions of the model, which are:

- the baseline fatigue crack growth rate reached before the application of the overload is  $(da/dN)_{\text{base}} = C \cdot (\Delta K)^m$ ,
- loading conditions:  $R, K_{\max}, K_{\text{ol}}, R_{\text{ol}}$ ,
- material yield stress  $\sigma_y$ ,
- dimensions and geometry of the specimen.

Our model gives this type of delay curve by a linear approximation of the evolution of the logarithm to base ten of the fatigue crack growth rate  $(da/dN)$  on segments  $AB$  and  $BC$ .

The equation of the first segment of cracking  $[AB]$  can be expressed as

$$\log_{10} \left( \frac{da}{dN} \right) = E \times (a - a_{\text{ol}}) + F \quad (4)$$

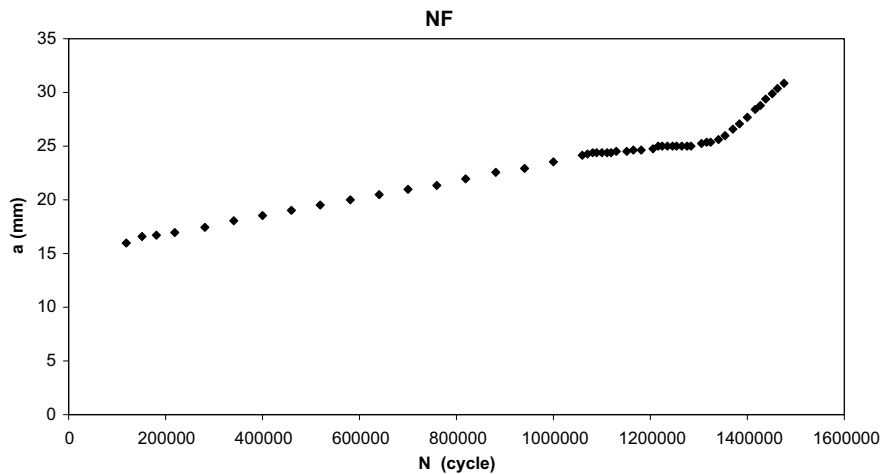


Fig. 5. Crack length a versus number of cycles  $N$  for two overloads.

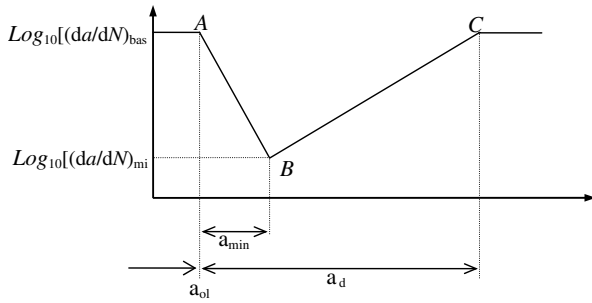


Fig. 6. Schematization of the delay model.

with  $E$  and  $F$  being respectively the directing coefficient and the ordinate at the origin of the first segment  $[AB]$ .

We have determined the delay coefficient  $C_d$  for a crack with length in the interval  $[a_{ol}; a_{ol} + a_{min}]$ :

$$C_d = (S_r)^{\left(\frac{a-a_{ol}}{a_{min}}\right)}. \tag{5}$$

The equation of the second segment of cracking  $[BC]$  can be expressed as

$$\log_{10}\left(\frac{da}{dN}\right) = G \times (a - a_{ol}) + H, \tag{6}$$

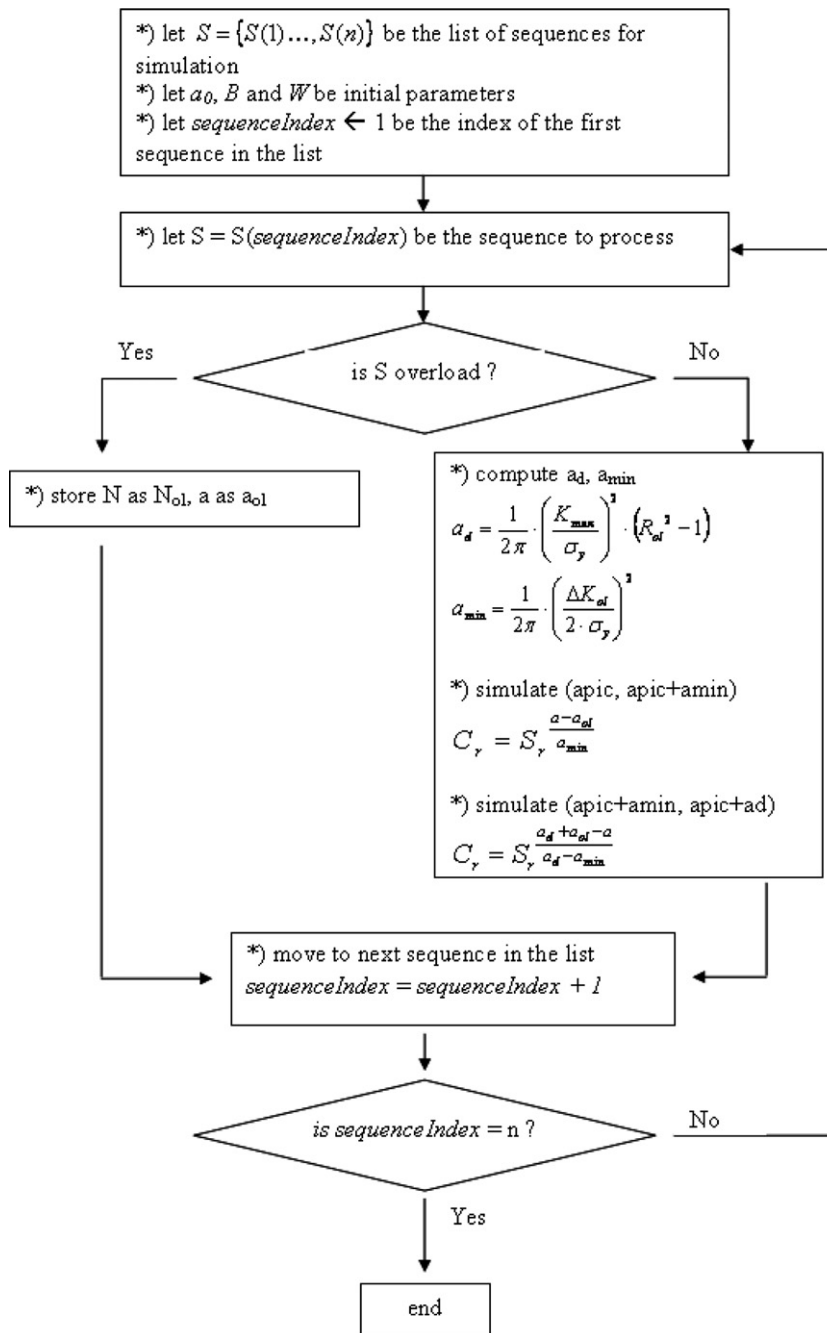


Fig. 7. Logical scheme of the program.

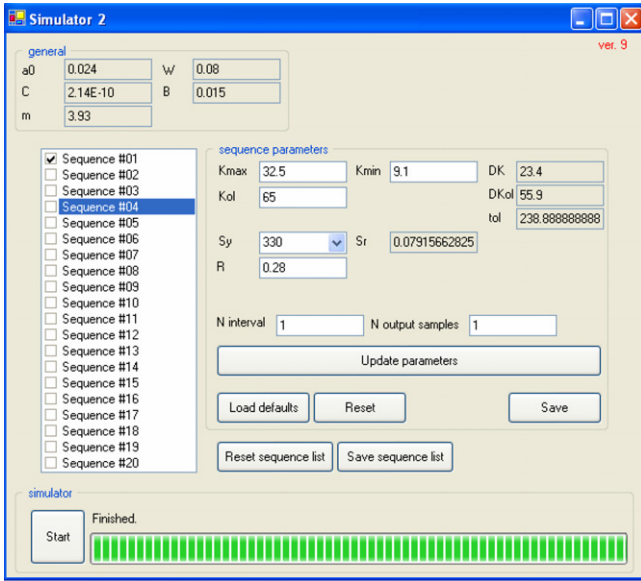


Fig. 8. Simulation program interface.

with  $G$  and  $H$  being respectively the directing coefficient and the ordinate at the origin of the second segment [BC].

The delay coefficient  $C_d$  for a crack with length in the interval  $[a_{ol} + a_{min}; a_{ol} + a_d]$  is given by

$$C_d = (S_r)^{\left(\frac{a_d + a_{ol} - a}{a_d - a_{min}}\right)}. \quad (7)$$

#### 4. Computer simulation concept

The computer simulation uses the mathematical model presented above.

The simulation process, carried out in C++ language, takes as input a list of sequences  $S = \{S(1), \dots, S(n)\}$  and a set of initial conditions ( $a_0$ ,  $B$  and  $W$ ). Each sequence is defined by a set of simulation parameters such as the mechanical properties of the material (the yield stress ( $\sigma_y$ ))

and Paris’s constants  $C$  and  $m$ ) and the loading conditions. These are the baseline loading ratio  $R$ , the baseline stress intensity factor range  $\Delta K (=K_{max} - K_{min})$ , the overload stress intensity factors  $K_{ol}$ ,  $R_{ol}$  and two extra parameters that control the output response in terms of sample points (maximum number of cycles and the output sample cycle interval). The output is given in terms of several simulated parameters such as  $da/dN$ ,  $a$ ,  $a - a_{ol}$ ,  $N$ ,  $N - N_{ol}$ ,  $F_{max}$ ,  $F_{min}$ ,  $a_d$ ,  $a_{min}$ .

The sequences are simulated taking into consideration the different situations that may appear:

1. Sequence with no overload,  $K_{ol} = 0$ . The simulation is completely defined by  $(da/dN)_{base}$  over a specified number of cycles.
2. Single overload occurs: an overload is defined as a sequence with one simulation cycle that has a non-zero value for  $K_{ol}$ . The output parameters are generated taking into account specific parameters for a single overload given by our model, such as:  $a_d = \frac{1}{2\pi} \cdot \left(\frac{K_{max}}{\sigma_y}\right)^2 \cdot (R_{ol}^2 - 1)$ ,  $a_{min} = \frac{1}{2\pi} \cdot \left(\frac{\Delta K_{ol}}{2 \cdot \sigma_y}\right)^2$ ,  $C_r = S_r^{a_{min}}$  and  $C_r = S_r^{a_d - a_{min}}$ , respectively.
3. Multiple overloads are superimposed: if multiple overload conditions are met (the current simulated  $da/dN$  is less than the initial  $(da/dN)_{base}$  at the moment the second overload appears), the following distinct cases are taken into consideration:

- $a_{d2} < a_{min1}$ , which means that the second overload is much smaller than the first and it does not influence the simulation output results. The simulation is carried out as if this additional overload had not occurred.
- $a_{min2} \geq a_{min1}$  and  $a_{d2} > a_{min1}$ ;  $a_{min2} > a_{min1}$  and  $a_{d2} < a_{d1}$ ;  $a_{min2} > a_{min1}$ ,  $a_{min2} < a_{d1}$  and  $a_{d2} > a_{d1}$ : for all these cases the second overload influences the simulation results according to the relative position of the

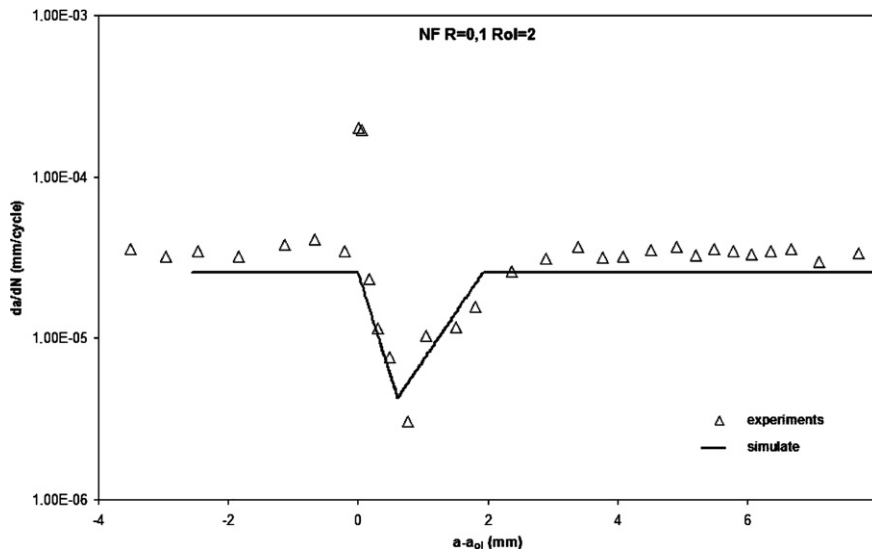


Fig. 9. Specimen with NF heat treatment.

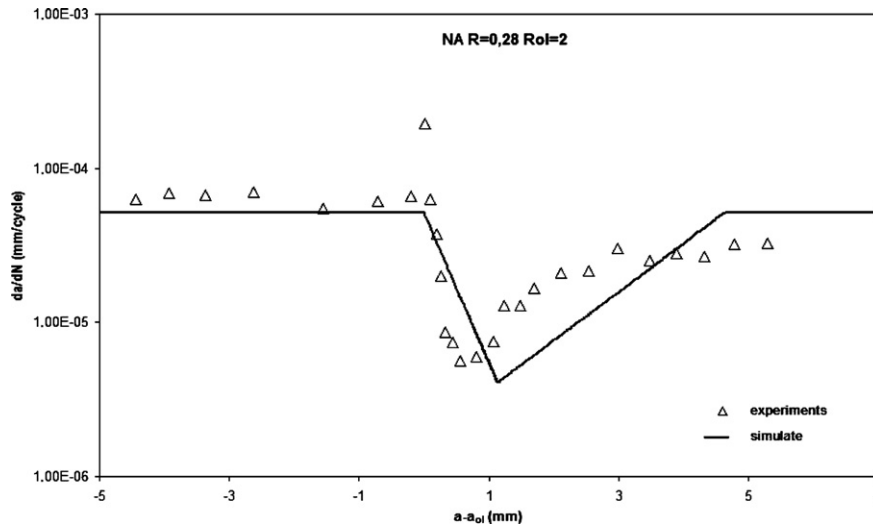


Fig. 10. Specimen with NA heat treatment.

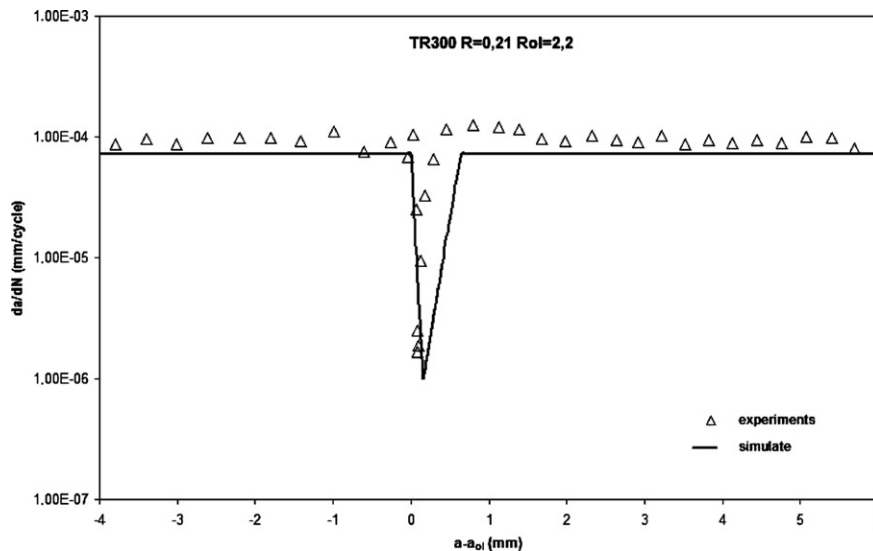


Fig. 11. Specimen with TR300 heat treatment.

points  $A_2$ ,  $B_2$ ,  $C_2$  of the second overload with respect to the points  $A_1$ ,  $B_1$ ,  $C_1$  of the first, where  $A$  is the position where an overload is applied;  $B$  is position of the minimum value of  $da/dN$  at a propagation value of  $a_{\min}$  and  $C$  is the position where  $da/dN$  is the same as the propagation speed at point  $A$ , at a relative propagation distance of  $a_d$ . Analyzing the relative positions of these points and handling properly the intersections of segments  $A_2B_2$  and  $B_1C_1$  will give the simulation results for the three distinct cases above.

The iteration calculus is shown in Fig. 7 and the user interface in Fig. 8.

The program has a user-friendly interface and accepts the multiple scenarios created by the various sequences.

## 5. Discussion and conclusions

The experimental results and the simulation were compared for the four types of specimens used in the experiments in the case of a single overload to validate the empirical model and the program. This comparison shows a good agreement (see Figs. 9–12).

The results of the simulations show that an overload applied at certain intervals of time leads to a temporary decrease in the advancement speed of the crack, and, overall, a series of overloads leads to an increase in the lifespan of a metallic sample before the crack reaches a critical limit.

We have obtained a good smooth curve for the case of sequential overload, which is shown in Fig. 13.

Overloads can produce a very short initial acceleration before significant deceleration occurs. This initial

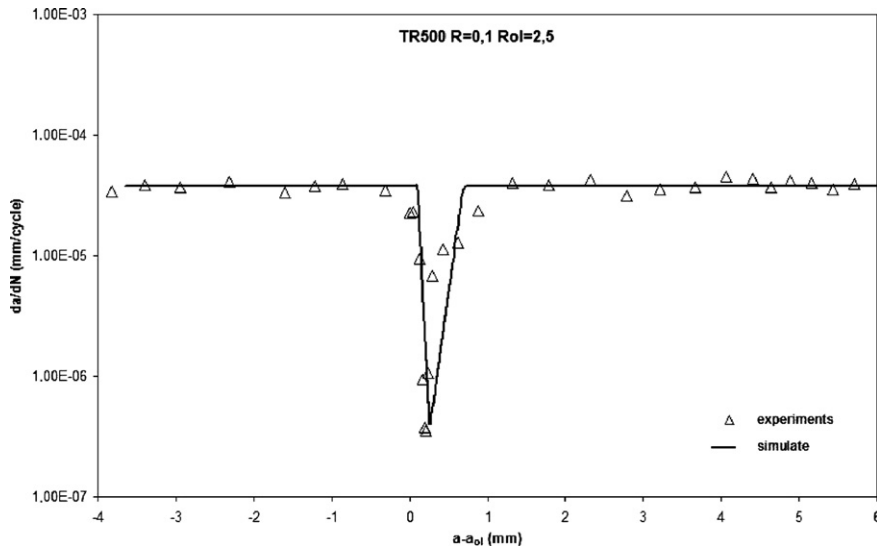


Fig. 12. Specimen with TR500 heat treatment.

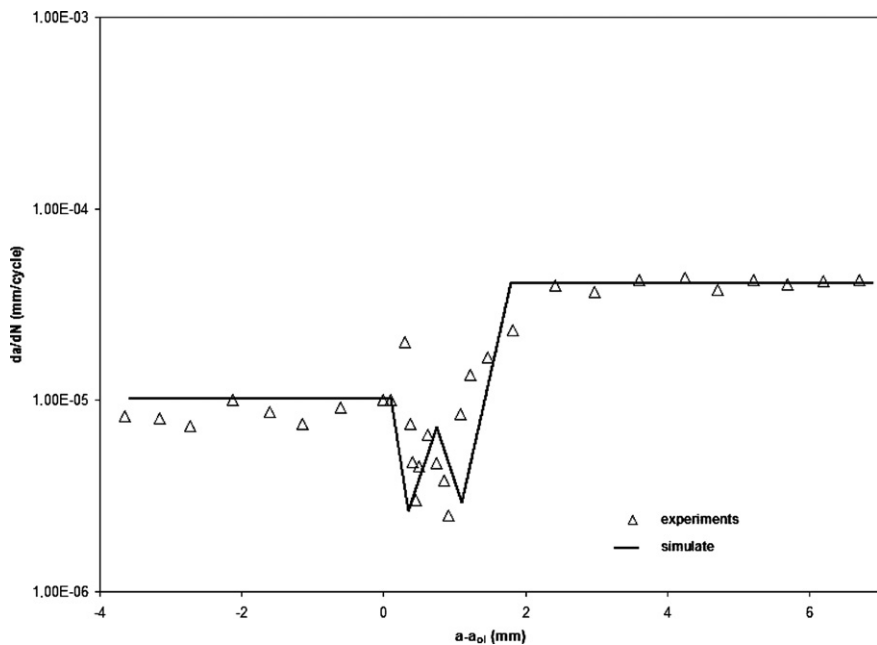


Fig. 13. Case of two consecutive overloads.

acceleration is observable only at high overload ratios and depends on the mechanical behaviour of the material. This can be seen clearly in a constant  $\Delta K$  test [9]. Our purpose was to create a computer simulation able to show the crack speed retardation after applying one or more overloads, and we ignored this initial acceleration.

### 5.1. Conclusions

- The computer simulation is able to predict the crack growth retardation for a single overload and two overloads with different initial speeds even when we had ignored the initial acceleration after the overload.
- It is shown that modifying the delay retardation causes an interaction between the two overload.
- We have proposed a simple model using the mechanical properties of the material (the yield stress  $\sigma_y$ , and Paris's parameters  $C$  and  $m$ ), which offers a good agreement with experiments after modifying the yield stress with different heat treatments. This good agreement suggests that this computer simulation could be used on other materials.
- The simulation based on the model can be used to predict fatigue crack growth under random loading. So, we can imagine that a random loading has a mean stress on a mean magnitude which can be used to

determinate the baseline fatigue crack growth rate. Thus, a random loading can be reduce to constant amplitude loading containing successively overload and underload cycles.

- The model should be widely applicable after this development.

## References

- [1] Wheeler O. Spectrum loading and crack growth. *J Basic Eng D* 1972;94:181–6.
- [2] Plumtree A, Shen G. Cyclic deformation and life prediction using damage mechanics. In: Krause AS, editor. *Constitutive laws of plastic deformation and fracture*. Netherlands: Kluwer Academic; 1990. p. 77–85.
- [3] Golos K, Ellyin F. Generalization of cumulative damage criterion to multilevel cyclic loading. *Theor Appl Fract Mech* 1987;7:169–76.
- [4] Petinov SV. Fatigue crack initiation and propagation: an inelastic strain energy approach. In: *ISOPE-96: Proceedings of the 6th International Offshore and Polar Engineering Conference*, vol. IV. Colorado: International Society of Offshore and Polar Engineers; 1996. p. 246–9.
- [5] Glinka G, Shen G, Plumtree A. A multiaxial fatigue strain energy density parameter related to the critical plane. *Int J Fatigue Fract Eng Mater Struct* 1994;18:37–46.
- [6] Kikukawa M, Jono M, Murata Y. Effect of mean stress and cumulative damage under service loadings including stresses below the fatigue limit. In: Ferratt F, Sturgeon JB, editors. *Materials, experimentation and design in fatigue*, Proceedings of Fatigue '81. Guildford: Westbury House; 1981. p. 308–17.
- [7] Yan X, Cordes TS, Vogel JH, Dindinger PM. A property fitting approach for improved estimates of small cycle fatigue damage. SAE Technical Paper Series No. 920665. Philadelphia: Society for Automotive Engineers; 1992.
- [8] Conle A, Topper TH. Overstrain effects during variable amplitude service history testing. *Int J Fatigue* 1980;2(3):130–6. PR, editors. *ASTM STP1411: application of automation technology in fatigue and fracture testing and analysis*, vol. 4. West Conshohocken: ASTM; 2002. p. 165–180.
- [9] Sadananda K, Vasudevan AK, Holtz RL, Lee EU. Analysis of overload effects and related phenomena. *Int J Fatigue* 1999;21: S233–46.
- [20] Sander M, Richard HA. Fatigue crack growth under variable amplitude loading. Part II: analytical and numerical investigations. *Fatigue Fract Eng Mater Struct* 2005;29:303–19.
- [21] Sheu BC, Song PS. Shaping exponent in Wheeler model under a single overload. *Eng Fract Mech* 1995;51(1):135–43.
- [22] Skorupa M, Skorupa A, Schjive J, Machniewicz T, Korbut P. Fatigue growth behavior of 18G2A steel under constant amplitude loading and following a single overload. *Arch Mech Eng* 2000;47:139–63.
- [24] Taheri F, Trask D, Pegg N. Experimental and analytical investigation of fatigue characteristics of 350WT steel under constant and variable amplitude loadings. *Mar Struct* 2003;16:69–91.
- [25] Lang M. A model of fatigue crack growth, part I: Phenomenology. *Fatigue Fract Eng Mater Struct* 2000;23:587–601.
- [26] Lang M. A model of fatigue crack growth, part II: Modelling. *Fatigue Fract Eng Mater Struct* 2000;23:603–17.